The Role of Micromixing in the Scale-Up of Geometrically Similar Batch Reactors

Richard W. Rice
Richard E. Baud
Department of Chemical Engineering
Clemson University
Clemson, SC 29634

Mixing is an important issue to consider during scale-up of many processes, particularly those involving batch reactors, but until relatively recently this topic has been largely based on empiricism. A contribution toward providing a more fundamental approach was made by J. R. Bourne and his colleagues through the development of both an experimental technique and an accompanying mathematical model for characterizing what is termed "micromixing" (Bourne et al., 1981; Angst et al., 1982). Unlike macromixing which is associated with large-scale fluid motions that can be monitored directly through physical property measurements, micromixing deals with diffusive mixing on the molecular level and only indirect methods are available for measuring it (Toor, 1970; Nauman, 1975; Ranz, 1979; Ottino, 1980; Angst et al., 1982; Villermaux and David, 1983; Bolzern and Bourne, 1983).

The importance of micromixing in terms of reactor design, scale-up and operation is most apparent when considering multiple reactions which are fast relative to mixing. Various fast, single-phase, competitive-consecutive (series-parallel) reactions of the general form shown in Eq. 1,

$$A + B \xrightarrow{k_1} R$$

$$R + B \xrightarrow{k_2} S, \qquad (1)$$

have been demonstrated (Paul and Treybal, 1971; Zoulalian and Villermaux, 1974; Bourne et al., 1981) to be mixing-influenced and, consequently, possible "probes" for monitoring micromixing. Bourne and others have made extensive use of the coupling reaction of 1-naphthol (A) with diazotized sulfanilic acid (B) in dilute aqueous solution to obtain a quantitative index of micromixing. This is the reaction used in the work reported here. The products, R and S, are 4-(4'-sulfophenylazo)-1 naphthol, and 2, 4 bis (4'-sulphophenylazo)-1 naphthol, both of which are dyestuffs. Measurement of the final concentrations, C_{R_f} and C_{S_f}, of the products enables calculation of a product distribution parameter,

$$X_S = \frac{2\,C_{S_f}}{2\,C_{S_f} + C_{R_f}} = \frac{\text{moles of } B \text{ consumed forming } S}{\text{total moles of } B \text{ consumed}}, \qquad (2)$$

which is a measure of the degree of segregation in the reaction zone.

A detailed description of the experimental aspects of utilizing this diazo coupling reaction for micromixing studies as well as a mathematical model that attempts to describe micromixing for the general conditions of the test reaction can be found in the literature (Angst et al., 1982; Baldyga and Bourne, 1984a,b,c), thus only a few relevant features will be described here.

The C_{R_f} and C_{S_f} values (and thus X_S) are functions of several dimensionless groups, of which the most pertinent for the work described here is the "mixing modulus," M, defined as,

$$M = \frac{k_2\,C_{B0}\,d_0^2}{D}, \qquad (3)$$

where C_{B0} is the initial molar concentration of B, d_0 is the initial half thickness of a fluid layer, and D is the diffusivity (assumed constant and equal for all species). The d_0 value can be related to the local rate of energy dissipation, E, through the equation,

$$d_0 = \frac{1}{2}\left[\frac{v^3}{E}\right]^{1/4}, \qquad (4)$$

where v is kinematic viscosity. For a stirred reactor, the local

Correspondence concerning this paper should be addressed to R. W. Rice.
R. E. Baud is now at Exxon Chemical Co., Baytown, TX.

rate of energy dissipation, E, can be related to the average energy dissipation rate, $\bar{E}$, via

$$E = \phi \bar{E} = \frac{\phi N_p N^3 D_a^5}{V_T} \tag{5}$$

where ϕ is a proportionality factor dependent on position, N_p is the impeller power number, N is the agitator speed, D_a is the impeller diameter, and V_T is the liquid volume in the vessel. The relevance of $\bar{E}$, to batch reactor scale-up is evident, because the average energy dissipation rate is simply the power input per unit volume divided by the fluid density, i.e., $\bar{E} = (P/V_T)/\rho$. Bourne's micromixing model predicts that for turbulent mixing in geometrically-similar vessels equal micromixing, i.e., X_S values, will be obtained during scale-up if the rate of energy dissipation in the reaction zone is held constant. Although E varies with position over two to three orders of magnitude (Baldyga and Bourne, 1984c; Bourne and Dell'Ava, 1987), ϕ depends only on position. This appears to suggest that during scale-up homologous feed points should be used and that the scale-up criterion for equivalent overall degree of micromixing will equal delivered power per unit fluid volume. However, as Bourne and Dell'Ava (1987) observed in comparing results for 2.5- and 66.3-L tanks, this is an overly simplistic view and valid only for specific feed points. The work described here was undertaken to gain a better understanding of how scale-up affects micromixing (or *vice versa*) in single-phase batch reactors and, in part, was effectively an extension of the work of Bourne and Dell'Ava to considerably larger scale-up ratios. In addition, a brief study was made of the effect of alterations in impeller and baffle design.

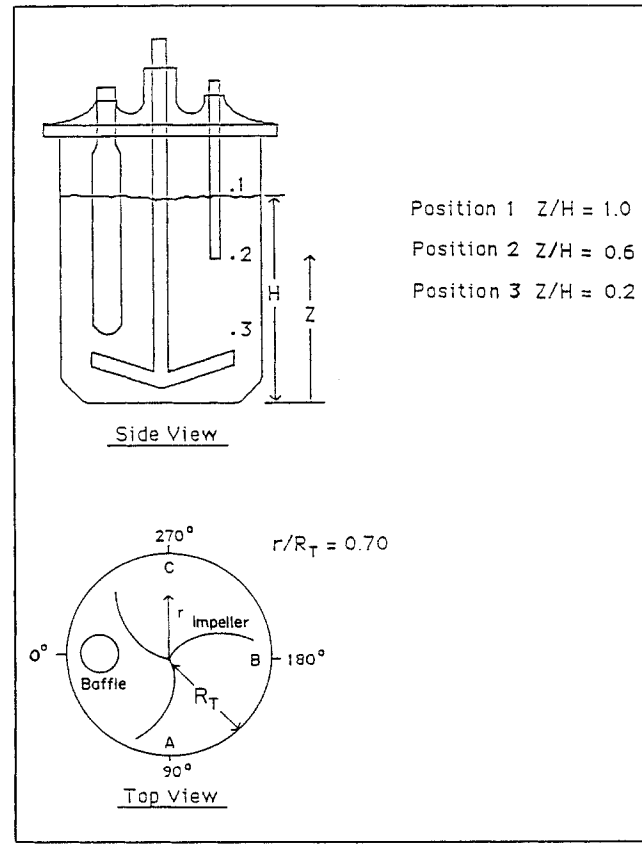

Figure 1. *B*-solution feed point location.

Experimental Studies

The experimental work was performed in the Unit Operations Research Laboratory at the Tennessee Eastman Co. in Kingsport, Tennessee. Tests were made using five approximately geometrically-similar Pfaudler-style batch reactors ranging in nominal (total empty) volume, V, from 3 to 2,650 L and in actual liquid (working) volume, V_T, from 1.5 to 2,293 L. Table 1 lists information concerning these reactors, and Figure 1 illustrates the general features of the reactors. Units T-3 and T-4 were actual glass-lined Pfaudler reactors with a single Pfaudler "h-style" baffle, while the other three reactors, MOD-1, T-1, and T-2, were made from laboratory glassware. In the smaller reactors, a single test tube (finger) baffle was used. All of the reactors contained geometrically-similar three-blade retreat curve impellers. A Heller 1/8-hp (93-W) motor and variable speed motor controller capable of speed and torque readings powered the impeller in the three laboratory reactors, while 2- and 5-hp (1.5- and 3.7-kW) motors equipped with adjustable frequency drives were used in the T-3 and T-4 reactors, respectively. An IBM Model 9430 UV/Visible spectrophotometer was used for reaction product analysis, and a Masterflex Digi-Staltic pump/flow controller was used for feeding *B* solution.

The reactant solutions were prepared in separate batches and used within six hours of preparation to prevent decomposition or contamination. For solution *A*, powdered 1-naphthol was dissolved in demineralized water to yield a concentration, C_{A0}, of 0.050 mol/m^3, and then the solution was buffered with sodium carbonate and sodium bicarbonate to achieve a pH in the range from 9.95 to 10.15. In preparing solution *B*, anhydrous sulfanilic acid was converted to diazotized sulfanilic acid by reaction with sodium nitrite and hydrochloric acid in aqueous solution and kept between 1°C and 5°C to prevent decomposition of the diazonium salt. The concentration of this solution was C_{B0} = 4.76 mol/m^3 with a pH between 2.45 and 2.55.

Table 1. Volumes and Dimension Ratios of the Experimental Mixing Vessels

Unit	Nominal Vol. V (L)	Working Vol. V_T (L)	Dimension Ratios* D_a/D_T	E_T/D_T	W_a/D_a	H/D_T	D_b/D_T
Mod-1	3	1.5	0.623	0.05	0.098	0.93	0.22
T-1	12	6.1	0.557	0.05	0.117	0.93	0.19
T-2	30	17.2	0.598	0.05	0.103	0.93	0.21
T-3	378	364.0	0.750	0.09	0.115	0.93	—
T-4	2,650	2,293.0	0.733	0.17	0.100	0.93	—

*Refer to Figure 1 and notation.

Essentially the same test procedure was used for each of the five reactors, and all runs were conducted at ambient pressure with the reactor temperature in the 22°C to 25°C range. In all cases, the volume ratio of A solution to B solution, (V_A/V_B), used was 100:1 giving an initial molar ratio (N_{A0}/N_{B0}) of 1.05, i.e., B was the limiting reagent. At the start of a run, the total specified volume, V_A, of 1-naphthol (A) solution was charged to the test reactor, the impeller speed was set at the desired value, and addition of B solution to the reactor at the desired pumping rate was carried out until a cumulative volume, V_B, had been delivered. The B solution was introduced to a given reactor through a feed tube positioned in one of the nine feed locations indicated in Figure 1. As described later, in most runs a three-point feed technique was used, wherein one third, i.e., $V_B/3$, of the B solution was added consecutively in three different locations. After the addition of the B solution was complete, a sample of the reactor contents was taken and the C_{R_f} and C_{S_f} values were determined using a UV/Visible spectrophotometer.

The analytical procedure used was that of Bourne et al. (1981). Each sample was scanned three to five times and the resulting average X_S value was used. The average standard deviation in X_S associated with this analysis was found to be ±0.0015 or ±3% around a mean X_S value of 0.05. Repeating runs at the same nominal conditions showed a run to run standard deviation in X_S of roughly ±10%, essentially equal to that reported by Bourne and Dell'Ava (1987). Material balance checks were made, assuming complete reaction of B to R and S, and averaged greater than 96% closure.

Power Number, N_p, values for each of the three laboratory reactors were determined experimentally. Attempts were made to measure N_p for the larger reactors (T-3 and T-4); but, because the no-load (empty reactor) torque value was roughly the same size as the "load" value, accurate measurements were not attainable, thus literature values furnished by Pfaudler were used.

Results and Discussion

Preliminary experiments

The two main items covered in preliminary experiments were:

1. The determination of power number for each of the five reactors

2. A study of X_S as a function of power dissipation when the B solution was fed at the A(reactor) solution upper surface

Measured N_p values ranged from 0.186 for the MOD-1 reactor to 0.590 for T-1. All mixing data were taken in the turbulent range ($N_{Re\,mix} > 10{,}000$). For the surface feeding runs, the X_S vs. E curves for the three laboratory reactors were relatively close to each other, but were markedly displaced from the curve predicted by the Bourne model, indicating ϕ values roughly an order of magnitude below 1.0. This is understandable since the actual reaction zone for the rapid test reaction was localized to a region immediately adjacent to the solution B feed point which was far from the impeller turbulence zone.

Multiposition feeding

Based on the surface feeding results, it was decided that a much better test of the micromixing model (and more accurate scale-up) required using a subsurface feed position for reactant B. Ideally, this position would be one for which the factor ϕ was approximately 1.0, i.e., one for which the local E value was representative of the reactor as a whole; for scale-up purposes, however, it would be adequate for the ϕ value, even if not 1.0, to be relatively constant for homologous feed positions.

In order to get an idea of how E, and thus ϕ, can vary within a stirred reactor, a series of runs was conducted in the intermediate sized T-2 reactor. Separate runs at a set agitator speed (150 rpm) and thus a constant $\bar{E}$ value were made in which the only variable was the feed point location. Nine different locations were examined, representing combinations of the three vertical positions (1, 2, 3) and three lateral positions (A, B, C) shown in Figure 1. The radial distance, $r/R_T = 0.70$, was chosen because, in an earlier series of experiments examining the variation in X_S with r/R_T at position $B2$, only a small (<6%) variation around the mean value at $r/R_T = 0.70$ had been observed for r/R_T values ranging from 0.5 to 0.8. Table 2 presents the results of the nine-run "mixing mapping" tests. While the lateral variation in X_S at a given vertical position was within experimental error, X_S varied appreciably with vertical position, with most efficient mixing occurring near the impeller. For the conditions of these runs, the average energy dissipation rate, $\bar{E}$, was 0.075 W/kg, a value which, when inserted into Bourne's model, yields a predicted X_S of 0.035. This is negligibly different from the level 2 ($Z/H = 0.6$) average, implying a ϕ value very near 1.0, whereas for level 1 (surface) and level 3 ($Z/H = 0.2$) estimates of ϕ based on the model were 0.096 and 3.33, respectively.

A complete characterization of the spatial dependence of micromixing effectiveness would have required performing similar nine-run series of experiments at numerous $\bar{E}$ values in each reactor and time constraints on the project precluded this. In addition, since the major thrust of the study required only that reproducible relative measures be obtained, it was felt that this series at a representative $\bar{E}$ value had adequately identified level 2 as a good choice for feed position. Accordingly, a three-point feed technique was made standard for subsequent runs. This technique involved feeding one third of the B solution at positions $A2$, $B2$, and $C2$, consecutively in a given run in order to get a composite average X_S value.

Micromixing scale-up runs

Given that each data point represents a separate run, Figure 2 summarizes data for over 50 three-point feed runs, roughly ten different runs in each of the five reactors. This plot shows that, although there are five distinctly identifiable curves rather than the ideal of a single curve, i.e., perfect scaling, the spread in the

Table 2. Results of "Micromixing Mapping" Experiments in Unit T-2 at N = 150 rpm and $\bar{E}$ = 0.075 W/kg

Feed B Location* (see Fig. 1)	Product Distribution Parameter, X_s	
$A1$	0.095	
$B1$	0.109	Avge. = 0.098
$C1$	0.090	
$A2$	0.033	
$B2$	0.040	Avge. = 0.036
$C2$	0.035	
$A3$	0.021	
$B3$	0.021	Avge. = 0.021
$C3$	0.022	

*All at $r/R_T = 0.70$.

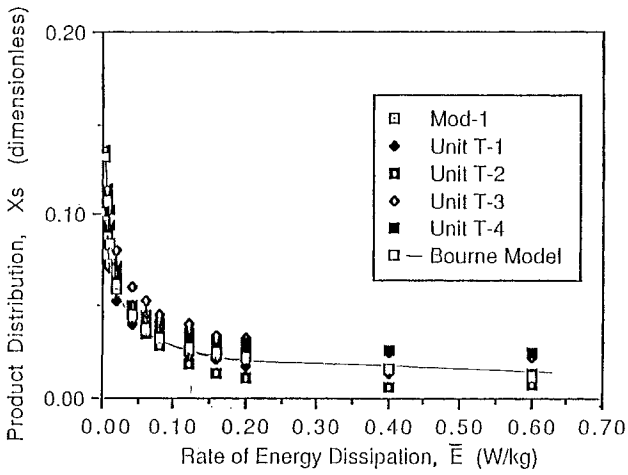

Figure 2. Micromixing scale-up results for three-point subsurface feeding (positions *A2*, *B2*, *C2*).

curves is not very large and the curves for the three laboratory reactors are quite close to the Bourne model predictions over most of the range of interest. The data do not show a monotonic trend of shifting upward or downward as the vessel size changes, but the curves for the two larger reactors (T-3 and T-4) do clearly fall above the model-predicted curve, suggesting that ϕ was appreciably less than unity for the reaction zones near the *A2*, *B2* and *C2* feed positions in these vessels. A likely explanation for this is related to what might be termed "further localization" of the test reaction zone in these larger vessels.

The circulation time in an agitated vessel is inversely proportional to the impeller speed, and the larger vessels were operated at appreciably lower speeds, thus for a given P/V_T or $\bar{E}$ value the larger tanks had a longer circulation time than the smaller tanks. This means that on a dimensionless basis the *B* solution after injection traveled through a smaller fraction of the reactor volume in the larger reactors. To get a semiquantitative comparison related to this, calculations were made of:

1. A characteristic time, t_{DR}, required for diffusion/reaction using Bourne's micromixing model for a representative $\bar{E}$ value of 0.12 W/kg (Bourne and Dell'Ava, 1987)

2. The (convective) transport time, t_T, of reactant *B* from the feed tube to the impeller

While t_{DR} is independent of reactor size and equal to 0.24 s at the specified condition for all five reactors, t_T increases with reactor size. Using the measure distances between the level 2 feed points and the impeller along with estimates of the average velocity of reactant *B* (Laufhutte and Mersmann, 1985), the estimated t_T values at this $\bar{E}$ value were roughly 0.4, 0.7, 0.8, 1.6 and 2.4 s, for the MOD-1, T-1, T-2, T-3 and T-4 reactors, respectively. Although $t_{DR} < t_T$ in all cases, i.e., reactant *B* is consumed before reaching the impeller, the t_T/t_{DR} ratio for the two largest reactors is 4 to 6 times that for the smallest one. Thus, it is concluded that the reaction zone in the smaller reactors incorporates regions closer to the impeller periphery where the higher energy dissipation (better micromixing) zones occur. Consequently, it is reasonable to assume that, were it not for the fact that the impeller to tank diameter ratio, D_a/D_T, was higher for the two large vessels than for the three smaller ones, the T-3 and T-4 curves in Figure 2 would lie even further above those for the smaller reactors.

Baffle and impeller geometry effects

A brief study was made to observe the effect on micromixing of changes in impeller width, impeller diameter, and the baffle system. A preliminary step in each case was the determination of power number, N_p, in order that $\bar{E}$ values could be calculated from measure N values. In all cases, the test reaction was run using the three point subsurface feed technique described earlier. The MOD-1 reactor was operated with an impeller with a blade width twice that of the standard impeller, and the effect was substantial. The X_S vs. E curve for the double-wide blade was consistently 0.02 X_S units below that for the standard blade, indicating an improvement in mixing effectiveness on a nominally-equal P/V_T basis. The standard blade results matched the Bourne model for $\phi \approx 1$, but the wide blade results implied a ϕ value of nearly 5. Apparently the wide blade impeller created a reaction zone with a local energy dissipation value much higher than the $\bar{E}$ value based on the power number; probably due to the t_T value being reduced by a factor of 1.5, allowing the *B* solution to reach the high turbulence zone at the impeller. Interestingly, X_S as a function of N went through a minimum (0.01) representative of nearly perfect mixing at $N \approx 500$ rpm and then increased somewhat at $N = 700$ and 900 rpm. This reproducible result is probably due to the extreme vortexing in this high N range causing the feed tube location to be nearly a surface-feed point, with a consequent lowering of ϕ relative to the lower N cases.

A second series of runs was made in the *T*-2 reactor to see the effect of using otherwise identical impellers with dimensionless diameter (D_a/D_T) values of 0.44, 0.60 (standard), and 0.75. Figure 3 summarizes the results, showing that micromixing effectiveness increased with increasing impeller diameter. As in the case just discussed, this variation in system geometry clearly altered the spatial distribution of energy dissipation such that the standard (*A2*, *B2*, *C2*) feed technique no longer created a reaction zone for which ϕ was approximately unity. For the largest and smallest impellers, ϕ would have to be adjusted to about 4.3 and 0.7, respectively, in order to align the data with Bourne's model. Again, this presumably reflects changes in pumping capacity (and thus t_T/t_{DR}) at a given $\bar{E}$ or P/V_T value. It is interesting to note that for the largest impeller the pumping capacity

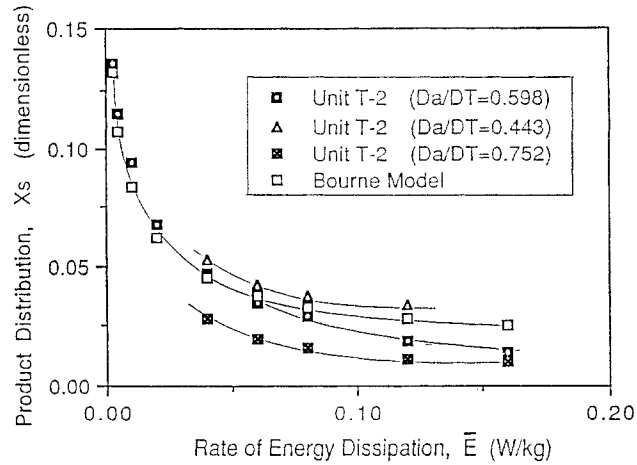

Figure 3. Effect of impeller diameter on micromixing in unit *T*-2 (V_T = 17.2 L).

was 45% larger than that for the standard impeller, which is comparable to the 50% increase for the double-wide MOD-1 impeller, and the apparent local energy dissipation factor, ϕ, values for the two cases were also comparable, 4.3 vs. 5, respectively.

Finally, runs were made in the T-2 reactor, in which the baffle system was radically altered relative to the standard single finger baffle. In one run, the reactor contained no baffle while in the other four full-height rectangular (slat) baffles ($D_b/D_T = 0.1$) located 90° apart were used. The power number for the no baffle case was 63% less than that for the standard finger baffle case, whereas for the four-slat baffle case it was 48% higher. The X_S vs. agitator speed, N, curves for these two cases were nearly the same as that for the standard case; but, as Figure 4 shows, the X_S vs. $\bar{E}$ curves are distinctly different. On a power input per unit volume basis, the no-baffle case provided the most effective micromixing and the four-slat baffle case gave the worst.

It is plausible that the slat baffle configuration provided a more balanced E distribution throughout the tank than did the no-baffle case in which extreme vortexing and less vertical mixing were encountered. However, apparently the three level-2 feed points used in this study introduced reactant B into a region of high local energy dissipation in the no-baffle case. A much more extensive mapping of the spatial variation of ϕ by using different vertical feed positions would be needed to gain a good understanding of the effect of baffle configuration on micromixing, but the effects are clearly significant enough to merit close attention during scale-up.

Acknowledgment

This work was supported by the Tennessee Eastman Company as part of the Graduate Residency Program of the Dept. of Chemical Engineering at Clemson University. The authors wish to thank V. L. Brown, M. R. Davis, E. Lockhart, J. N. Schlather, and M. P. Wolford, of Tennessee Eastman for their assistance.

Notation

A = reactant in series-parallel test reaction, specifically 1-naphthol or its ionized form, Eq. 1

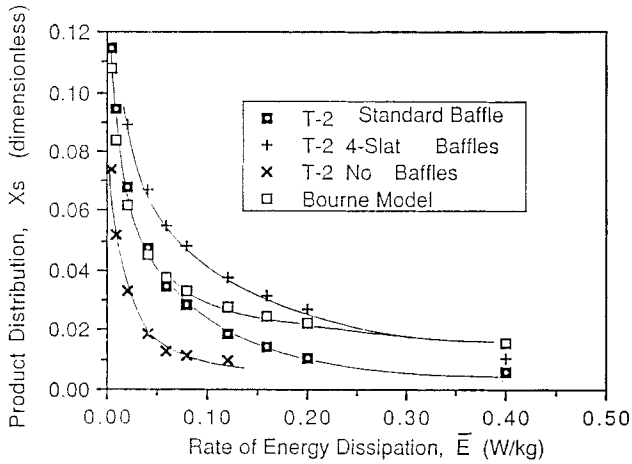

Figure 4. Effect of baffle configuration on micromixing in unit T-2.

B = reactant in series-parallel test reaction, specifically diazotized sulfanilic acid or its ionized form, Eq. 1
C_{A0}, C_{B0} = initial concentrations of reactants A and B, respectively
C_{Rf}, C_{Sf} = final concentrations of species R and S, respectively
d_0 = initial half thickness of a fluid layer in Bourne's model, Eq. 4
D = diffusivity
D_a = impeller diameter
D_b = baffle diameter (or width)
D_{FT} = inside diameter of feed tube
D_T = inside diameter of reactor
E = local energy dissipation rate, Eq. 5
$\bar{E}$ = reactor average energy dissipation rate
E_T = impeller clearance off reactor bottom
g = gravitational acceleration
H = liquid height in reactor
k_1, k_2 = pH-dependent rate constants for the primary and secondary reaction steps
M = micromixing modulus, Eq. 3
N = impeller speed
N_{A0}, N_{BD} = initial number of moles of reactants A and B, respectively
N_p = power number
$N_{Re,\,mix}$ = mixing Reynolds number = $N D_a^2/\lambda$
P = power imparted to fluid
r = radial distance
R = primary product in test reaction, Eq. 1
R_T = inside radius of reactor
S = secondary product in test reaction Eq. 2
t_D = characteristic time for diffusion
t_{DR} = characteristic time for combined diffusion and reaction
t_R = characteristic time for reaction *per se*
t_T = convective transport time for reactant B from feed tube to the impeller
V = total nominal reactor volume
V_A, V_B = volume of A and B solutions, respectively
V_T = actual fluid volume in reactor
W_a = width of impeller blade
X_S = product distribution parameter, Eq. 2
Z = vertical distance from reactor bottom

Greek letters

υ = kinematic viscosity
ϕ = proportionality constant relating average and local energy dissipation rates
ρ = fluid density

Literature Cited

Angst, W., J. R. Bourne, and R. N. Sharma, "Mixing and Fast Chemical Reaction-IV, The Dimensions of the Reaction Zone," *Chem. Eng. Sci.*, **37**, 585 (1982).

Baldyga, J., and J. R. Bourne, "A Fluid Mechanical Approach to Turbulent Mixing and Chemical Reaction: 1. Inadequacies of Available Methods," *Chem. Eng. Commun.*, **28**, 231 (1984a).

———, "A Fluid Mechanical Approach to Turbulent Mixing and Chemical Reaction: II. Micromixing in the Light of Turbulence Theory," *Chem. Eng. Commun.*, **28**, 243 (1984b).

———, "A Fluid Mechanical Approach to Turbulent Mixing and Chemical Reaction: III. Computational and Experimental Results for the New Micromixing Model," *Chem. Eng. Commun.*, **28**, 259 (1984c).

———, "Mixing and Fast Chemical Reaction: VI. Extension of the Reaction Zone," *Chem. Eng. Sci.*, **38**, 999 (1983).

Bourne, J. R., unpublished data (1986).

Bourne, J. R., F. Kozicki, and P. Rys, "Mixing and Fast Chemical Reaction-I, Test Reactions to Determine Segregation," *Chem. Eng. Sci.*, **36**, 1643 (1981).

Bourne, J. R., and P. Dell'Ava, "Micro-and Macromixing in Stirred Tank Reactors of Different Sizes," *Chem. Eng. Res. Des.*, **65**, 180 (1987).

Kramers, H., "Physical Factors in Chemical Reaction Engineering," *Chem. Eng. Sci.*, **8**, 45 (1958).
Laufhutte, H. D., and A. Mersmann, "Dissipation of Power in Stirred Vessels," Paper No. 33, European Conf. on Mixing, Wurzburg, 331 (1985).
Mao, K. W., and H. L. Toor, "A Diffusion Model for Reactions with Turbulent Mixing," *AIChE J.*, **16**, 49 (1970).
McCabe, W. L., J. C. Smith, and P. Harriott, *Unit Operations of Chemical Engineering*, 4th ed., 222, McGraw-Hill, New York (1985).
Nauman, E. B., "The Droplet Diffusion Model for Micromixing," *Chem. Eng. Sci.*, **30**, 1135 (1975).
Ottino, J. M., "Lamellar Mixing Models for Structured Chemical Reactions and Their Relationship to Statistical Models, Macro- and Micromixing and the Problem of Averages," *Chem. Eng. Sci.*, **35**, 1377 (1980)
Paul, E. L., and R. E. Treybal, "Mixing and Product Distribution for a Liquid-Phase Second Order, Competitive-Consecutive Reaction," *AIChE J.*, **17**, 718 (1971).
Ranz, W. E., "Application of a Stretch Model to Mixing, Diffusion, and Reaction in Laminar and Turbulent Flows," *AIChE J.*, **25**, 41 (1979).
Villermaux, J., and R. David, "Recent Advances in the Understanding of Micromixing Phenomena in Stirred Reactors," *Chem. Eng. Commun.*, **21**, 105 (1983).
Zoulalian, A., and J. Villermaux, "Influence of Chemical Parameters on Micromixing in a Continuous Stirred Tank Reactor," *ACS Adv. Chem. Ser.*, **133**, 348 (1974).

Manuscript received May 30, 1989, and revision received Nov. 13, 1989.